Numerical Modeling of Earthquake Motions: Waves and Ruptures
June 30 - July 4, 2019, Smolenice Castle near Bratislava, Slovakia

FDTD MODELLING OF SEISMIC WAVE PROPAGATION IN POROUS MEDIA

David **GREGOR** Peter **MOCZO** Jozef **KRISTEK** Josep **DE LA PUENTE**

Comenius University Bratislava, Slovakia Slovak Academy of Sciences, Bratislava, Slovakia Barcelona Supercomputing Center, Spain

Abstract

We have developed a discrete representation of a strong material heterogeneity in the poroelastic medium and poroviscoelastic medium in the low-frequency regime. The representation makes it possible to model an arbitrary shape and position of an interface with sub-cell resolution on a uniform spatial grid. The computational efficiency of the finite-difference grid is unchanged compared to the scheme for a homogeneous or smoothly heterogeneous medium because the number of operations for updating stress-tensor, fluid pressure and particle velocities is the same. The only difference is that it is necessary to evaluate averaged grid material parameters once before the finite-difference simulation itself. The developed representation extends the possibilities of the finite-difference modelling of seismic wave propagation in the poroelastic medium.

We numerically demonstrate accuracy and sub-cell resolution of our modelling on a variety of canonical models by comparing the finite-difference solutions with analytical solutions and also an independent numerical method. We also present preliminary results of investigating effects of presence of a porous water-saturated sediment layer (described by a depth of a water table, porosity and permeability) in local surface sedimentary basins on earthquake ground motion characteristics.

2D P-SV constitutive law and equations of motion
for the poroelastic medium

$$\begin{bmatrix}\sigma_{xx}\\ \sigma_{zz}\\ \sigma_{xz}\\ -p\end{bmatrix}=\begin{bmatrix}\Lambda+\alpha^2M & \lambda+\alpha^2M & 0 & \alpha M\\ \lambda+\alpha^2M & \Lambda+\alpha^2M & 0 & \alpha M\\ 0 & 0 & 2\mu & 0\\ \alpha M & \alpha M & 0 & M\end{bmatrix}\begin{bmatrix}\varepsilon_{xx}\\ \varepsilon_{zz}\\ \varepsilon_{xz}\\ \varepsilon_{w}\end{bmatrix}$$

$$\begin{bmatrix}\dot v_x\\ -\dot q_x\\ \dot v_z\\ \dot q_z\end{bmatrix}=\frac{1}{\dfrac{\rho}{\rho_f}-\dfrac{\rho_f}{m}}\begin{bmatrix}\frac{1}{\rho} & \frac{1}{m} & \frac{b}{m} & 0 & 0 & 0\\ \frac{1}{m} & \frac{\rho}{\rho_f}\frac{1}{m} & \frac{\rho}{\rho_f}\frac{b}{m} & 0 & 0 & 0\\ 0 & 0 & 0 & \frac{1}{\rho} & \frac{1}{m} & \frac{b}{m}\\ 0 & 0 & 0 & \frac{1}{m} & \frac{\rho}{\rho_f}\frac{1}{m} & \frac{\rho}{\rho_f}\frac{b}{m}\end{bmatrix}\begin{bmatrix}\sigma_{xx,x}+\sigma_{xz,z}\\ p_{,x}\\ q_x\\ \sigma_{zz,z}+\sigma_{xz,x}\\ p_{,z}\\ q_z\end{bmatrix}$$

- $\sigma_{xx}, \sigma_{zz}, \sigma_{xz}$ total stress-tensor components
- p fluid pressure
- $\varepsilon_{xx}, \varepsilon_{zz}, \varepsilon_{xz}$ solid matrix strain-tensor components
- w_x, w_z ; $\varepsilon_w \equiv w_{x,x}+w_{z,z}$ components of displacement of the fluid relative to the solid frame
- $\Lambda \equiv \lambda + 2\mu$ Lamé elastic coefficients of the solid matrix
- α poroelastic coefficient of effective stress
- M coupling modulus between the solid and fluid
- v_x, v_z solid particle velocities
- q_x, q_z fluid particle velocities relative to the solid
- ρ, ρ_f total and fluid densities
- m mass coupling coefficient
- b resistive friction

boundary conditions at an interface between poroelastic media

continuity of the

- $\sigma_{ij}^{+} n_j = \sigma_{ij}^{-} n_j$ traction vector
- $p^{+} = p^{-}$ fluid pressure
- $u_i^{+} = u_i^{-}$ solid displacement vector
- $w_i^{+} n_i = w_i^{-} n_i$ normal component of the relative fluid displacement vector

velocity-stress finite-difference staggered-grid cell

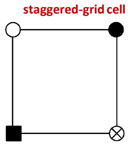

- ■ $v_x^{m+1/2}$, $q_x^{m+1/2}$ — ρ, ρ_f, m, b
- ● $v_z^{m+1/2}$, $q_z^{m+1/2}$
- ⊗ σ_{xx}^{m} , σ_{yy}^{m} , σ_{zz}^{m} , p^{m} — $\lambda, \Lambda, \alpha, M$
- ○ σ_{zx}^{m} — μ

2D P-SV constitutive law and equations of motion
for the averaged poroelastic medium

$$\begin{bmatrix}\sigma_{xx}\\ \sigma_{zz}\\ \sigma_{xz}\\ -p\end{bmatrix}=\begin{bmatrix}XX+\frac{XP\,XP}{\Psi} & XZ+\frac{XP\,ZP}{\Psi} & 0 & \frac{XP}{\Psi}\\ XZ+\frac{XP\,ZP}{\Psi} & ZZ+\frac{ZP\,ZP}{\Psi} & 0 & \frac{ZP}{\Psi}\\ 0 & 0 & 2\langle\mu\rangle^{Hx} & 0\\ \frac{XP}{\Psi} & \frac{ZP}{\Psi} & 0 & \frac{1}{\Psi}\end{bmatrix}\begin{bmatrix}\varepsilon_{xx}\\ \varepsilon_{zz}\\ \varepsilon_{xz}\\ \varepsilon_{w}\end{bmatrix}$$

$$\begin{bmatrix}\dot v_x\\ -\dot q_x\\ \dot v_z\\ -\dot q_z\end{bmatrix}=\begin{bmatrix}\frac{\langle F^x\rangle^z}{\langle S^x\rangle^z} & \frac{\langle G^x\rangle^z}{\langle S^x\rangle^z} & \frac{\langle H^x\rangle^z}{\langle S^x\rangle^z} & 0 & 0 & 0\\ \frac{\langle R^x\rangle^z\left\langle\frac{G^x}{R^x}\right\rangle^z}{\langle S^x\rangle^z} & \frac{\langle P^x\rangle^z\langle G^x\rangle^z}{\langle S^x\rangle^z} & \frac{\langle P^x\rangle^z\langle H^x\rangle^z}{\langle S^x\rangle^z} & 0 & 0 & 0\\ 0 & 0 & 0 & \frac{\langle F^z\rangle^x}{\langle S^z\rangle^x} & \frac{\langle G^z\rangle^x}{\langle S^z\rangle^x} & \frac{\langle H^z\rangle^x}{\langle S^z\rangle^x}\\ 0 & 0 & 0 & \frac{\langle R^z\rangle^x\left\langle\frac{G^z}{R^z}\right\rangle^x}{\langle S^z\rangle^x} & \frac{\langle P^z\rangle^x\langle G^z\rangle^x}{\langle S^z\rangle^x} & \frac{\langle P^z\rangle^x\langle H^z\rangle^x}{\langle S^z\rangle^x}\end{bmatrix}\begin{bmatrix}\sigma_{xx,x}+\sigma_{xz,z}\\ p_{,x}\\ q_x\\ \sigma_{zz,z}+\sigma_{xz,x}\\ p_{,z}\\ q_z\end{bmatrix}$$

where, for example,

$$XX=\left\langle\left\langle\Lambda-\frac{\lambda^2}{\Lambda}\right\rangle^{z}+\left\langle\frac{\lambda}{\Lambda}\right\rangle^{z\,2}\langle\Lambda\rangle^{Hz}\right\rangle^{Hx}\qquad F^{\xi}=\frac{1}{\langle\rho_f\rangle^{\xi}}$$

$$XZ=\left\langle\frac{\lambda}{\Lambda}\right\rangle^{xz}\langle\Lambda\rangle^{Hxz}\qquad H^{\xi}=\frac{\langle b\rangle^{\xi}}{\langle m\rangle^{\xi}}$$

$$\Psi=\left\langle\frac{1}{M}+\frac{\alpha^2}{\Lambda}\right\rangle^{xz}-\left(\left\langle\frac{\alpha}{\Lambda}\right\rangle^{xz}\right)^2\langle\Lambda\rangle^{Hxz}\qquad S^{\xi}=\frac{\langle\rho\rangle^{\xi}}{\langle\rho_f\rangle^{\xi}}-\frac{\langle\rho_f\rangle^{\xi}}{\langle m\rangle^{\xi}}$$

Numerical tests

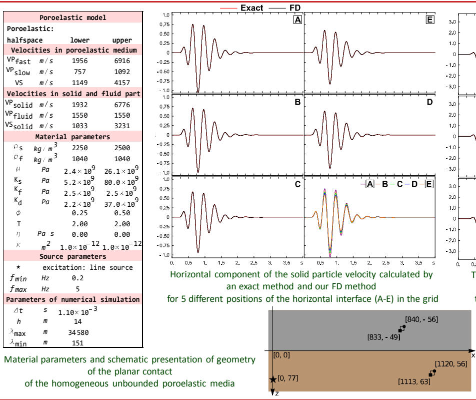

Horizontal component of the solid particle velocity calculated by an exact method and our FD method for 5 different positions of the horizontal interface (A-E) in the grid

The right panel corresponds to receiver above interface and the left panel corresponds to receiver below interface

Material parameters and schematic presentation of geometry of the planar contact of the homogeneous unbounded poroelastic medium

5 positions of the horizontal planar interface in the grid labeled A, B, C, D and E

Labels A and E are framed in order to indicate that the distance between the two positions is just one grid spacing h

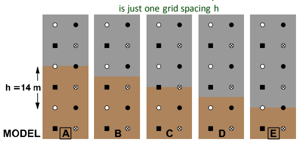

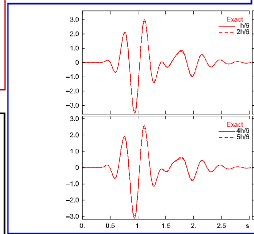

Horizontal component of the solid particle velocity calculated by an exact method and our FD method for two couples of positions of the interface in the grid shown in the Figure to the right

4 different positions of interface in the grid Considering position A (figure above) as a reference, the 4 positions are at distances h/6, 2h/6, 4h/6 and 5h/6, h meaning the grid spacing, downward from position A

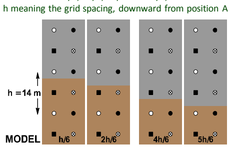

5 positions of the planar interface in the grid differing in the angle between the interface and horizontal grid line.

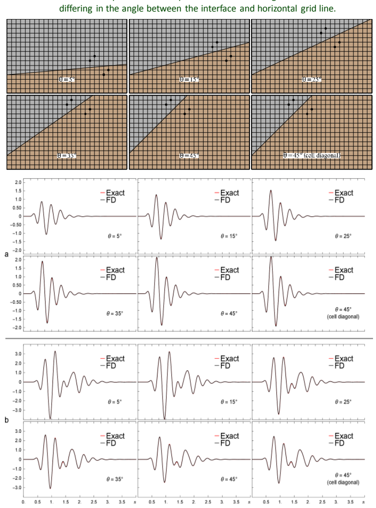

Horizontal component of the solid particle velocity calculated by an exact method (in red) and our FD method (in black)

The upper panel labelled **a** is for receiver above interface and the lower panel labelled **b** is for receiver below interface

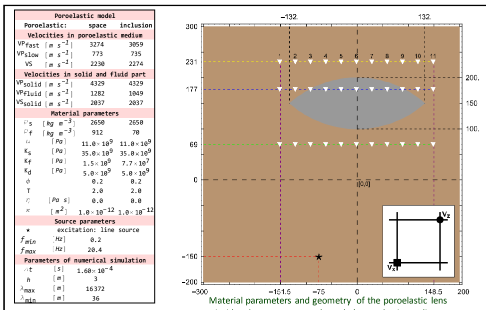

Material parameters and geometry of the poroelastic lens inside a homogeneous unbounded poroelastic medium

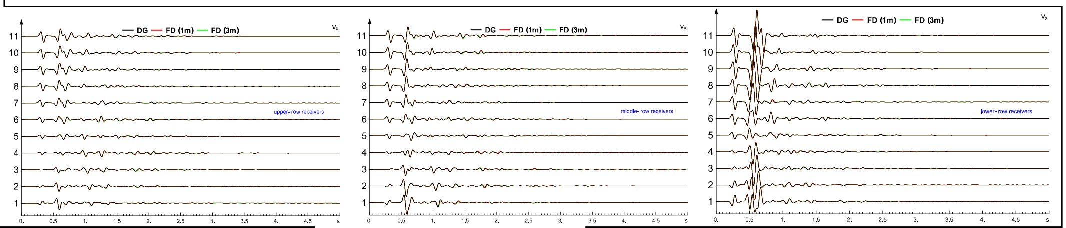

Horizontal component of the solid particle velocity (upper, middle and lower-row receivers) calculated by the discontinuous Galerkin method (DG in black) and our FD method (grid spacings 1 m in red and 3m in green)

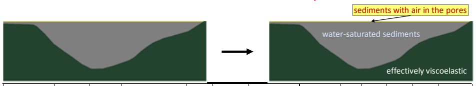

Model name	Unit	Depth range		Type of medium	Pore fluid	Porosity	Permeability	Biot's frequency	Q_S	Q_{K_d}	VP	VS	ρ
		m					m^2	Hz			m/s	m/s	kg/m^3
d1f1 pve -10	1	0	5	poro-viscoelastic	air	0.21	10^{-10}	1704	23	∞	960	230	2100
	2	5	160	poro-viscoelastic	water	0.27	10^{-10}	186	60	∞	240	600	2200
	bedrock	∞		elastic					∞	∞	4000	1500	2500
d1f2 pve -10	1	0	5	poro-viscoelastic	air	0.21	10^{-10}	1704	23	∞	960	230	2100
	2	5	160	poro-viscoelastic	water	0.21	10^{-10}	113	60	∞	2344	586	2307
	bedrock	∞		elastic					∞	∞	4000	1500	2500
d1f3 pve -10	1	0	5	poro-viscoelastic	air	0.27	10^{-10}	2790	23	∞	1002	240	1928
	2	5	160	poro-viscoelastic	water	0.27	10^{-10}	186	60	∞	2400	600	2200
	bedrock	∞		elastic					∞	∞	4000	1500	2500
d1f4 pve -10	1	0	5	poro-viscoelastic	air	0.37	10^{-10}	4788	23	∞	1077	258	1667
	2	5	160	poro-viscoelastic	water	0.39	10^{-10}	346	60	∞	2512	628	2008
	bedrock	∞		elastic					∞	∞	4000	1500	2500
d4f1 pve -10	1	0	5	poro-viscoelastic	air	0.21	10^{-10}	1704	23	∞	960	230	2100
	2	5	640	poro-viscoelastic	water	0.27	10^{-10}	186	60	∞	2400	600	2200
	bedrock	∞		elastic					∞	∞	4000	1500	2500
d4f2 pve -10	1	0	5	poro-viscoelastic	air	0.21	10^{-10}	1704	23	∞	960	230	2100
	2	5	640	poro-viscoelastic	water	0.21	10^{-10}	113	60	∞	2344	586	2307
	bedrock	∞		elastic					∞	∞	4000	1500	2500

Because we have
an efficient and sufficiently accurate
representation of heterogeneity of the poro-viscoelastic medium

we can apply this representation
also to
models with viscoelastic and poro-viscoelastic parts

Effect of water–saturated sediments
on amplification and aggravation factors of the cumulative absolute velocity

d4f2 pve -10

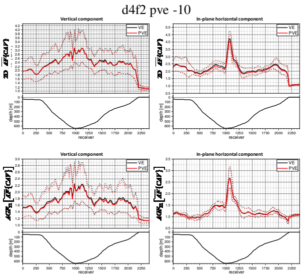

Conclusions

we have developed

a discrete representation of heterogeneity

of the poroelastic medium

this representation is

another proof that

the most advanced FD schemes

are powerful tools

for numerical modelling

of seismic wave propagation

References

Moczo, Kristek, Gális 2014 The Finite-difference Modelling of Earthquake Motions: Waves and Ruptures
Cambridge University Press

Kristek, Moczo, Chaljub, Kristekova 2017 An orthorhombic representation of a heterogeneous medium for the finite-difference modelling of seismic wave propagation
Geophys. J. Int. 208, 1250–126

Kristek, Moczo, Bard, Hollender, Stripajová 2018 Computation of Amplification Factor of Earthquake Ground Motion for a Local Sedimentary Structure
Bull. Earthq. Eng. 16, 2451-2475

Moczo, Kristek , Bard , Stripajová, Hollender, Kristeková, Chovanová, Sicilia 2018 Key Structural Parameters Affecting Earthquake Ground Motion in 2D and 3D Sedimentary Structures
Bull. Earthq. Eng. 16, 2421-2450

Moczo, Gregor, Kristek, de la Puente 2019 A discrete representation of material heterogeneity for the finite-difference modelling of seismic wave propagation in a poroelastic medium
Geophys. J. Int. 216, 1072-1099.

Kristek, J., Moczo, P., Chaljub, E. & Kristekova, M., 2019 A discrete representation of a heterogeneous viscoelastic medium for the finite-difference modelling of seismic wave propagation
Geophys. J. Int., in press.

Acknowledgements

This work was supported in part by the Slovak Research and Development Agency, APVV-15-0560 (project ID-EFFECTS).

Part of the calculations were performed in the Computing Centre of the Slovak Academy of Sciences using the supercomputing infrastructure acquired in project ITMS 26230120002 and 26210120002 (Slovak infrastructure for high-performance computing) supported by the Research and Development Operational Programme funded by the ERDF.

Dávid Gregor was supported by the junior Comenius University in Bratislava Grant UK3242017